

Supplementary Information

A new material discovery platform of the stable layered oxides cathode for K-ion batteries

Sohyun Park,^{a,‡} Sunhyeon Park,^{a,‡} Young Park,^{a,‡} Muhammad Hilmy Alfaruqi,^{a, b} Jang-Yeon Hwang,^{*,a} and Jaekook Kim^{*,a}

^a Department of Materials Science and Engineering, Chonnam National University, Gwangju 61186, South Korea

^b Department of Metallurgical Engineering, Sumbawa University of Technology, West Nusa Tenggara, 84371, Indonesia

Author Information

‡ These authors contribute equally to this work.

Corresponding Author

*E-mail: hjy@jnu.ac.kr; jaekook@chonnam.ac.kr

Experimental Section

Material preparation. The P'3-type $K_{0.3}MnO_2$ and $K_{0.3}Cu_{0.1}Mn_{0.9}O_2$ were synthesized using a polyol-assisted pyro-synthesis according to our previous work.^{1,2} First, potassium nitrate (Sigma-Aldrich, 99%), manganese(II) nitrate tetrahydrate (Sigma-Aldrich, 97%), and copper(II) nitrate trihydrate (Sigma-Aldrich, 99%) were dissolved in 75 ml of tetra-ethylene glycol (ACROS, 99.5%) and stirred for 3 h to obtain a transparent solution. An inflammable liquid thinner was added to the precursor solution and then stirred for 30 min. The obtained solution was ignited using a torch to induce a self-extinguishable combustion reaction on a hot plate at 450 °C. The as-prepared powder was annealed in muffle furnace at 800 °C for 12 h to obtain crystalline KMCO materials. The KMO material were synthesized through the same route without the Cu precursor.

ML & DFT calculation. The ML model used the latest updated the Materials Project dataset. In addition, implementing this artificial neural network ML model may also produce different values when implementing *random seed* due to, for example, random initialization of weights and biases.³⁻⁵ First-principles calculations based on density functional theory were performed using the Quantum Espresso (version 6.3) package.⁶ Electronic structures were calculated using the projector augmented wave (PAW) pseudopotential and the revised version for solids of the Perdew–Burke–Ernzerhof (PBEsol) within the generalized gradient approximation (GGA) exchange-correlation functional.⁷ A plane-wave basis set with a kinetic energy of 37 Ry (503 eV) was set. All the atoms within the $3 \times 2 \times 1$ supercell (containing 12 transition metal, 24 oxygen, and a varied number of K depending on the K concentration) and the corresponding lattice parameters was allowed to relaxed using the the Broyden–Fletcher–Goldfarb–Shanno (BFGS) algorithm with an energy convergence and force convergence of 1×10^{-4} Ry and 1×10^{-3} Ry Bohr, respectively. The Brillouin zone was sampled using a k-point of $1 \times 2 \times 2$. For DOS calculations, the Hubbard correction U of 3.9 eV was added for Mn.⁸ In addition, the grimme-d3 functional was implemented to take account of the physical van der Waals interaction for the H₂O molecule adsorption simulations.⁹ Crystal structures were drawn using the VESTA software.¹⁰

Material characterization. The elemental compositions of the samples were characterized via inductively coupled plasma-optical emission spectroscopy (ICP-OES) analysis using a PerkinElmer 4300 DV analyzer. The electronic conductivity of materials was characterized using a four-point probe (CMT-SR2000N). The

crystalline structure of the materials was studied via X-ray diffraction (XRD) using the Synchrotron XRD on the 9B-HRPD beamline at the Pohang Accelerator Laboratory. The materials powder was scanned from 10° to 130° with step size 0.01° while rotating the sample, and monochromated to the wavelength of 1.5212 \AA by a double-crystal Si (111) monochromater. The morphologies of the materials were characterized by field emission-SEM, Hitachi S-4700, and high-resolution-TEM, FEI Tecnai F20. Electrochemical impedance spectroscopy (EIS) was employed between 10 mHz and 1 MHz, (Bio-Logic VMP-3 electrochemical workstation). The synchrotron X-ray absorption near edge structure (XANES) measurements were performed at the BL-8C beamline of the Pohang Light Source (PLS). X-ray photoelectron spectroscopy (XPS) analysis was performed using Thermo VG Scientific Instrument, Multilab 2000 at Chonnam National University Center for Research Facilities (CCRF).

Electrochemical characterization. For the electrochemical measurements, the working electrodes were prepared by mixing the active material, ketjen black, and polyvinylidene fluoride (PVDF) in N-methylpyrrolidone (NMP) (ratio of 8:1:1). Then, the slurry was uniformly coated on a carbon-coated Al foil, which served as a current collector, and dried overnight under vacuum at 120°C . The dried foil was then hot-pressed between stainless steel twin rollers (maintained at 120°C) and punched into round discs (14 mm). The average loading weight of active materials on electrodes after drying was $1\text{--}2 \text{ mg cm}^{-2}$. A CR 2032-type coin cell was assembled in an Ar-filled glove box using the KMO and KMCO electrode with K metal as the counter electrode in 0.5 M KPF_6 in ethylene carbonate/diethylene carbonate (EC/DEC) with a 1:1 volume ratio. Galvanostatic electrochemical charge and discharge tests were run between 1.5 V and 3.9 V (vs K/K^+) at different current densities. Cyclic voltammetry was performed on the coin cells and they were assembled in an Ar-filled glove box using a programmable battery tester (TOYO) and Bio-Logic Science Instruments.

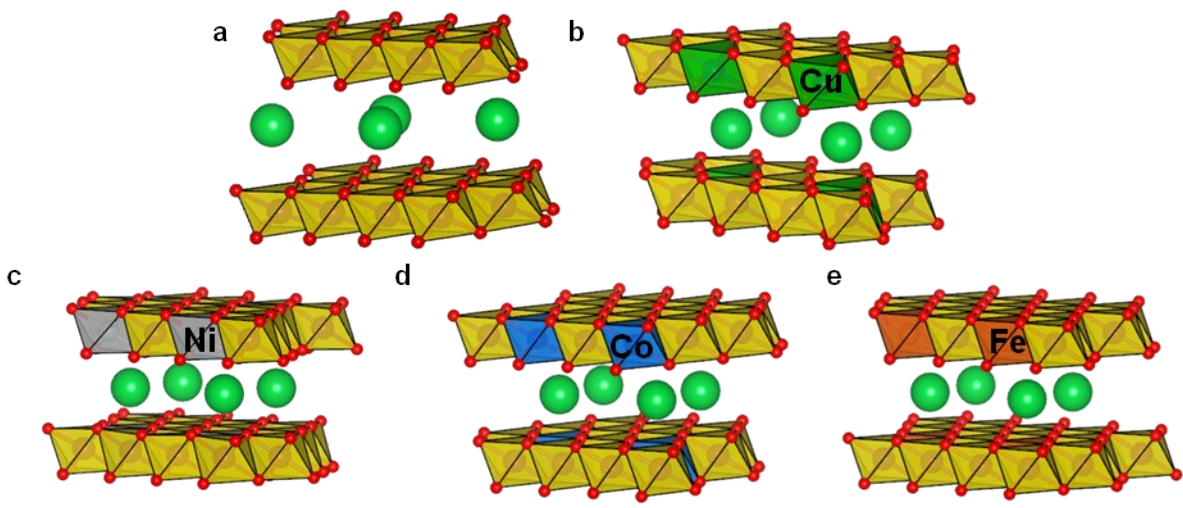


Fig. S1 The optimized structures using DFT calculation of (a) KMO, (b) Cu - KMO (c) Ni - KMO (d) Co - KMO (e) Fe - KMO.

ML algorithm	R²	RMSE
LR	0.848	0.36
DTR	0.83	0.38
ETR	0.945	0.21
MLP	0.956	0.19

Table S1 Performance metrics of ML models.

Table S2 ML-predicted formation energy per atom and their corresponding DFT-calculated α and γ angles.

Doping level	Dopant	ML-predicted Formation Energy per Atom	DFT-calculated α angle	DFT-calculated γ angle
0	Mn	-1.901	90	90
	Co	-1.917	90.0820	89.9783
	Ni	-1.892	90.0483	89.6619
	Fe	-1.903	90.0632	89.9719
	0.1	Cu	-2.026	89.6688
	Bi	-1.712	Not converged	Not converged
	Al	-2.076	Not converged	Not converged
	Zn	-1.985	Not converged	Not converged
0.2	Co	-1.887	Not converged	Not converged
	Ni	-1.837	90.064	89.812
	Fe	-1.881	90.053	89.952
	Cu	-1.901	90.176	89.857
	Bi	-1.690	89.496	90.078
	Al	-2.161	90.057	89.963
	Zn	-1.980	90.005	89.932

	K	Mn	Cu
KMO	0.299	1	0
KMCO	0.306	0.9	0.1

Table S3 ICP results of KMO and KMCO.

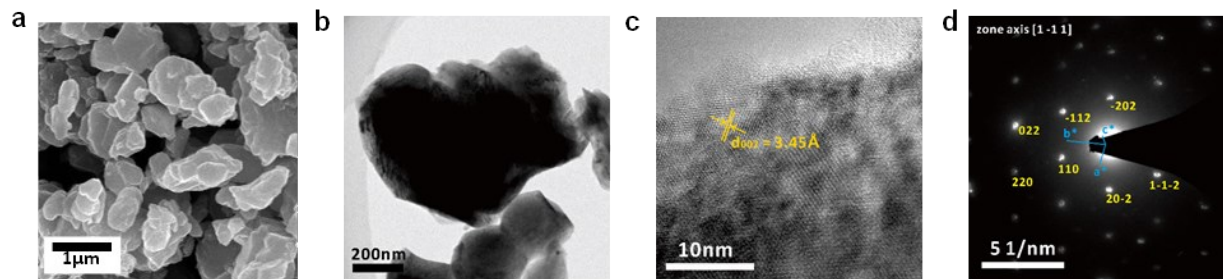


Fig. S2 Microscopic analysis of KMO particle. (a) SEM image (b) TEM image (c) The (002) plane of HR-TEM images and (d) SAED pattern.

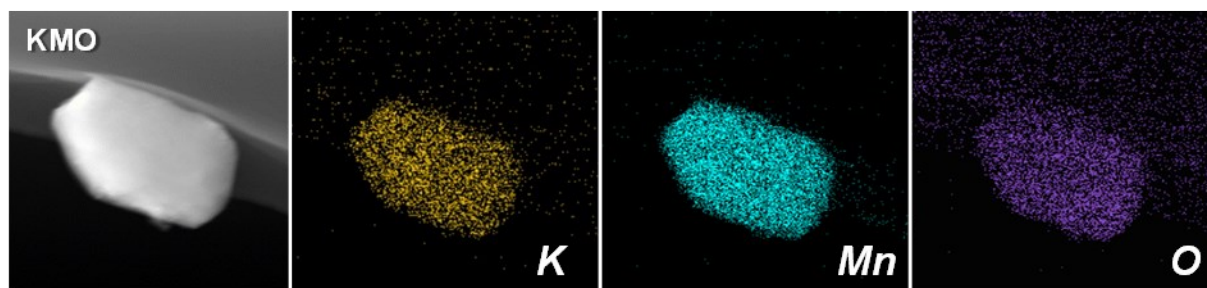


Fig. S3 EDS mapping analysis of KMO. (Yellow: K, Cyan: Mn, Purple: O).

Table S4 Lattice parameter and atomic position obtained from Rietveld refinement for KMO.

	a	b	c	α	β	γ
KMO	5.1263	2.8501	7.1525	90	101.96	90
Atom	#	Site	X	Y	Z	SOF
K	K⁺	4i	0.76913	0	0.48852	0.3239
Mn	Mn³⁺	2a	0	0	0	0.43195
Mn	Mn⁴⁺	2a	0	0	0	0.56805
O	O²⁻	4i	0.34171	0	0.11792	1

Table S5 Lattice parameter and atomic position obtained from Rietveld refinement for KMCO.

	a	b	c	α	β	γ
KMCO	5.0722	2.8676	7.1556	90	102.5	90

Atom	#	Site	X	Y	Z	SOF
K	K⁺	4i	0.73105	0	0.48906	0.32699
Mn	Mn³⁺	2a	0	0	0	0.26255
Mn	Mn⁴⁺	2a	0	0	0	0.63745
Cu	Cu²⁺	2a	0	0	0	0.1
O	O²⁻	4i	0.37622	0	0.13307	1

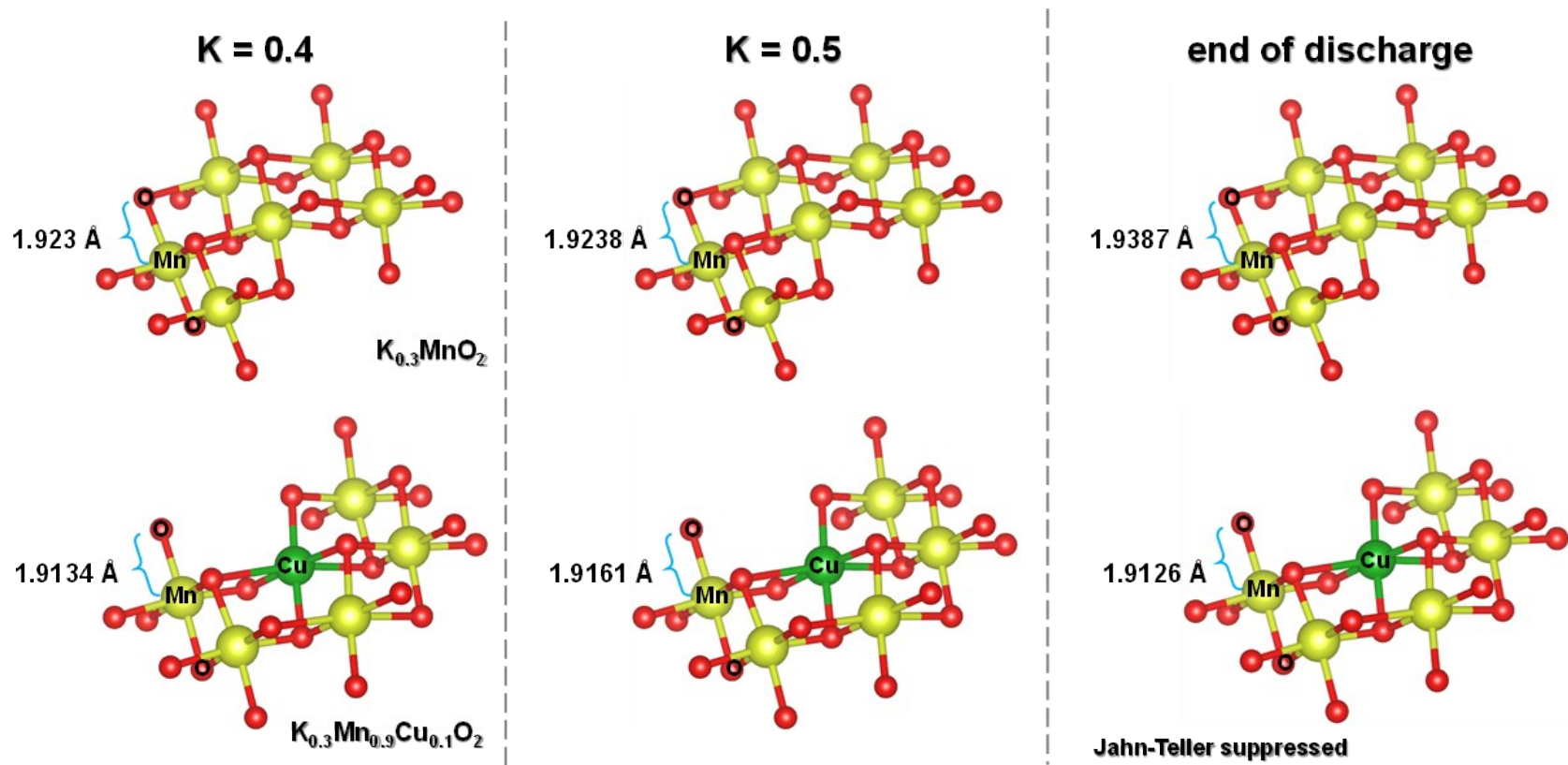


Fig. S4 Crystal structure of KMO and KMCO in discharge state with their corresponding the average TM-O bond lengths.

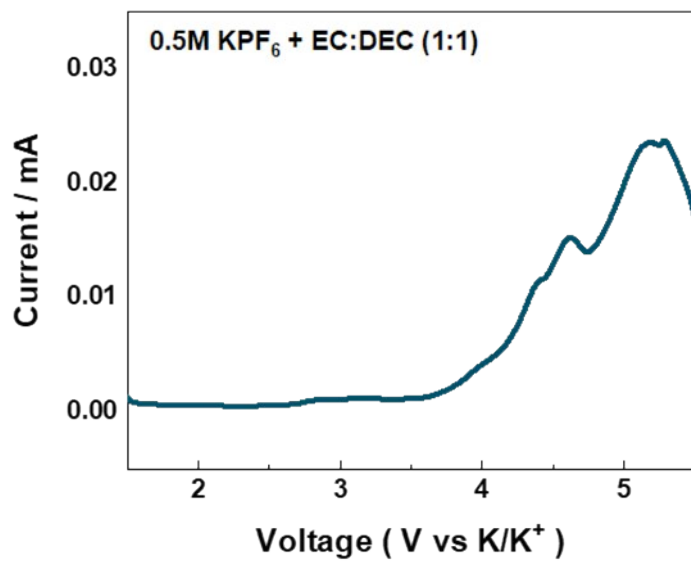


Fig. S5 Linear sweep voltammetry (LSV) of 0.5M KPF₆ / EC: DEC (1:1) electrolyte at a scan rate of 0.1 mV s⁻¹.

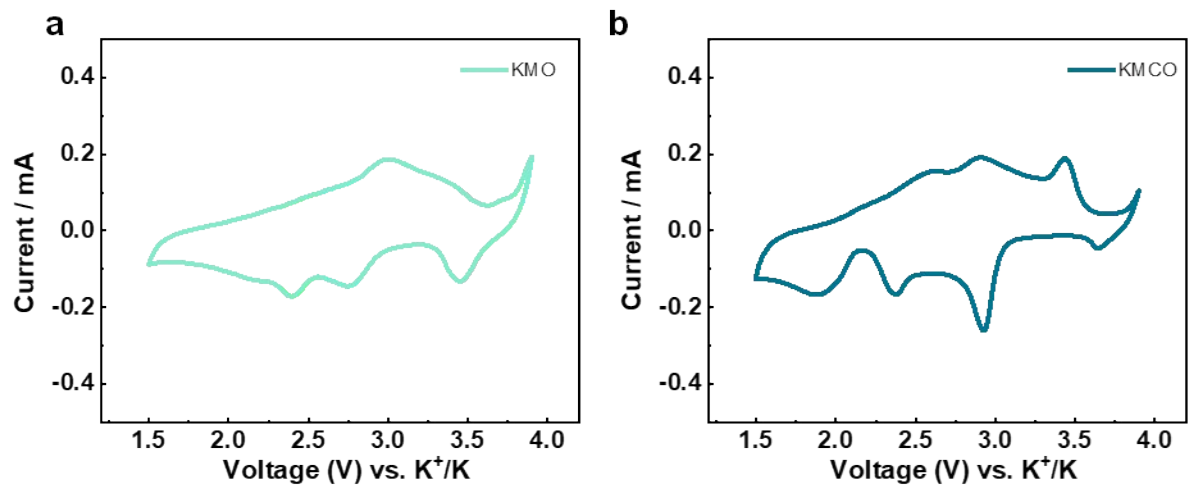


Fig. S6 CV curve of (a) KMO and (b) KMCO at scan rate of 0.2mV s^{-1} .

Table S6 d-orbital occupation numbers and the oxidation state (OS) of the Cu from DFT calculation.

Sample	Spin	Occupation numbers (d-orbitals)					OS
KMCO	1	0.709	0.718	0.996	0.998	0.998	Cu(III)
	2	0.971	0.982	0.998	1	1	

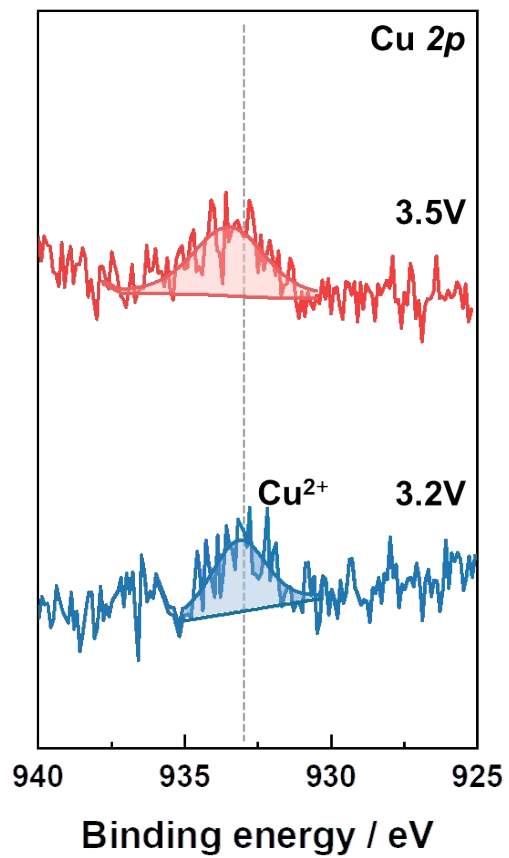


Fig. S7 Ex situ XPS spectra for Cu 2p at 3.2 V and 3.5 V of charge state.

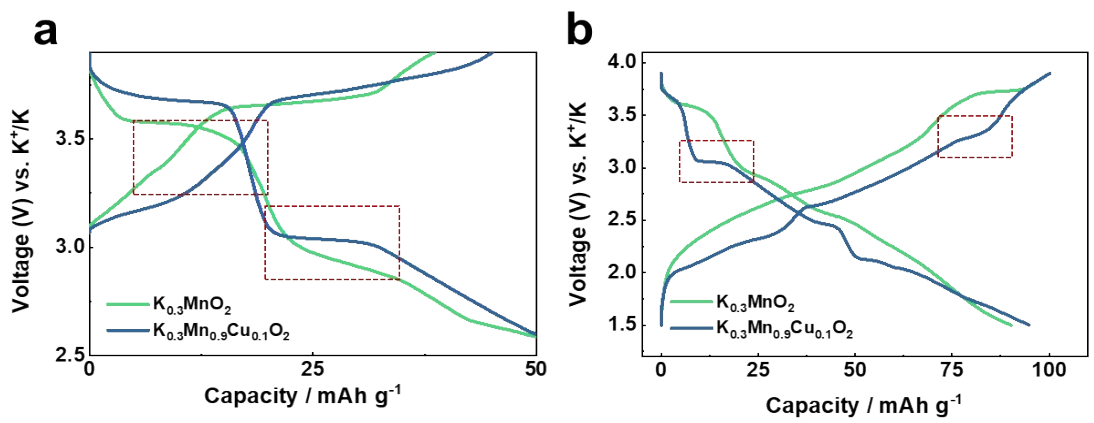


Fig. S8 (a) Magnified 1st charge-discharge curves and (b) 2nd charge-discharge curves of KMO and KMCO at 10 mA g⁻¹.

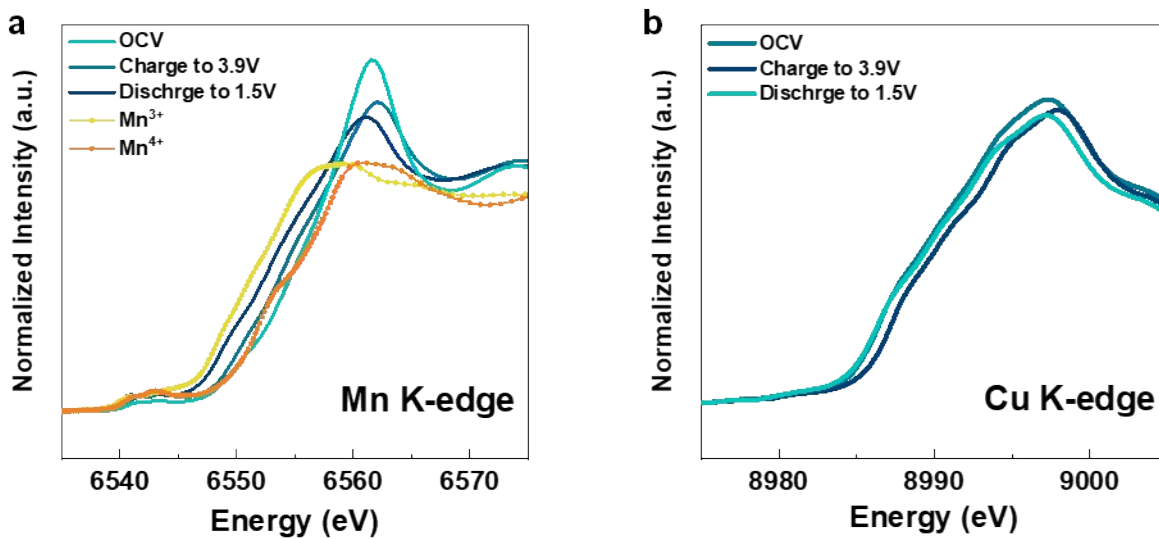


Fig. S9 (a) Mn K-edge ex-situ XANES spectra of KMCO (ref. Mn₂O₃, MnO₂), and (b) Cu K-edge ex-situ XANES spectra of KMCO.

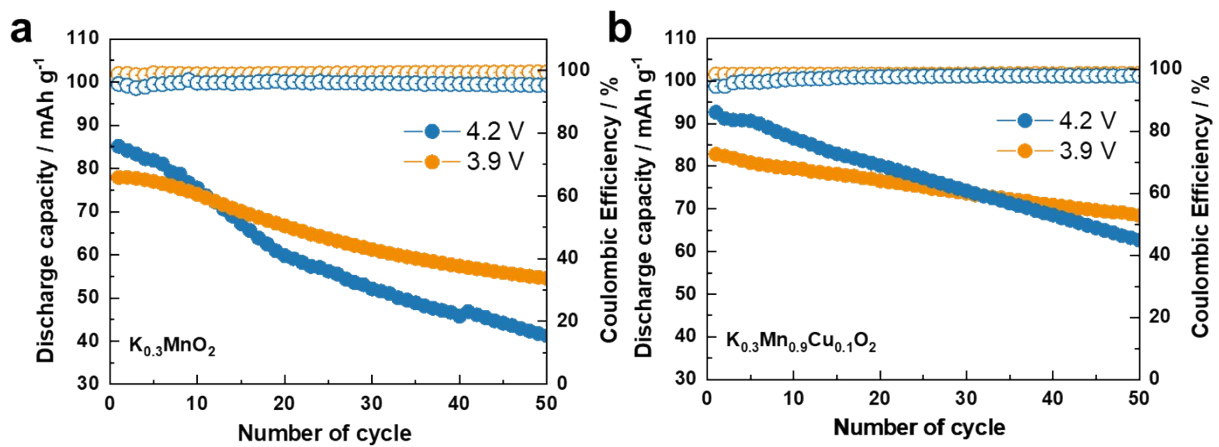


Fig. S10 Cycle life test of (a) KMO and (b) KMCO in a voltage range of 1.5-3.9 V and 1.5-4.2 V at a current density of 100 mA g⁻¹.

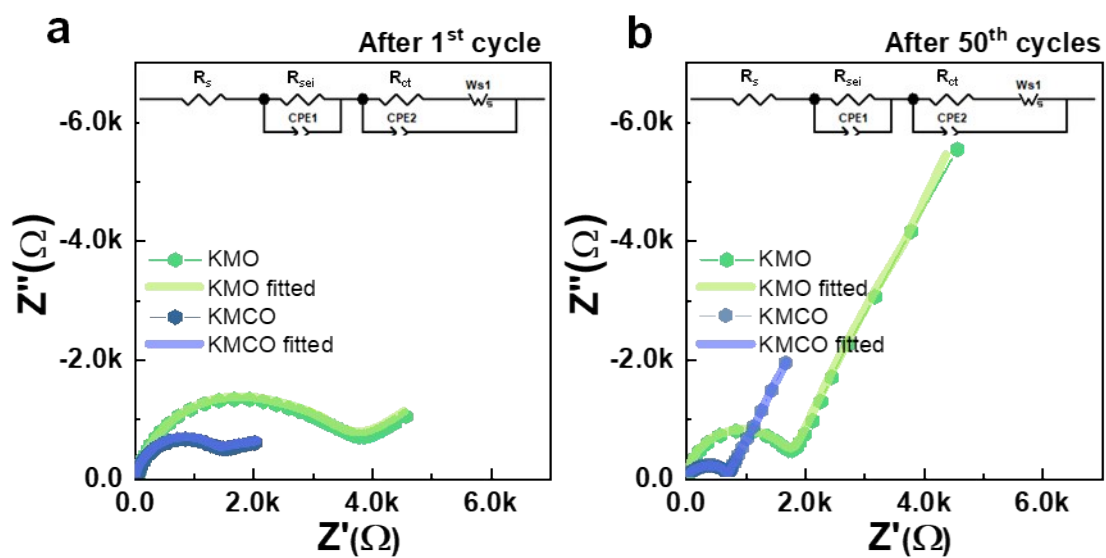


Fig. S11 Electrochemical impedance spectroscopy (EIS) of KMO and KMCO after (a) 1st cycle and (b) 50th cycles.

Table S7 The fitting data from EIS spectra using the equivalent circuit shown in Figure S11.

	Cycle	R_s (Ω)	R_{sei} (Ω)	R_{ct} (Ω)
KMO	1 st	5.94	161.9	3242
	50 th	6.873	917	2233
KMCO	1 st	5.93	130.9	1533
	50 th	4.985	233.9	473.2

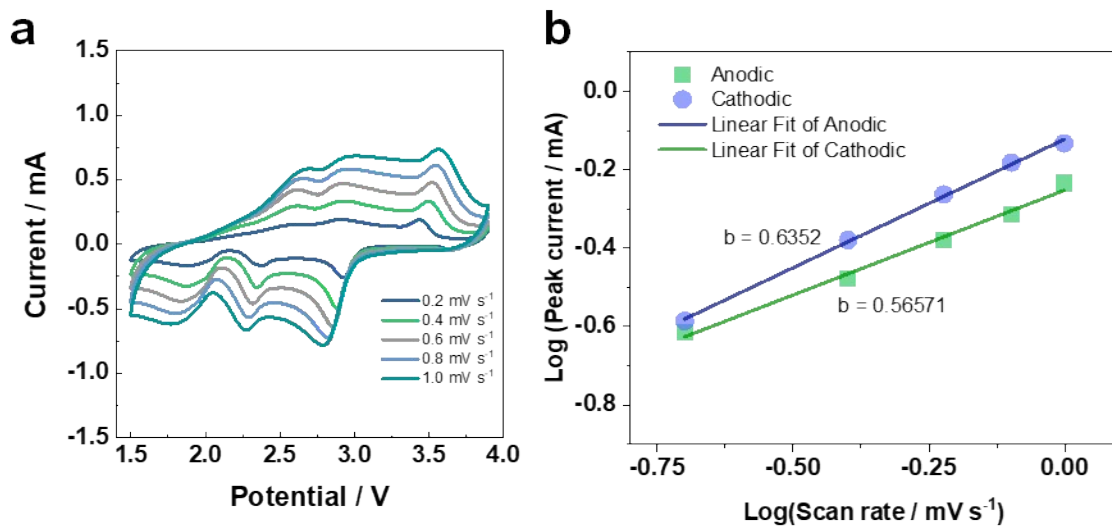


Fig. S12 (a) Multi-scan CV profile of KMCO at various scan rates, and (b) capacity contribution ratios at different scan rates.

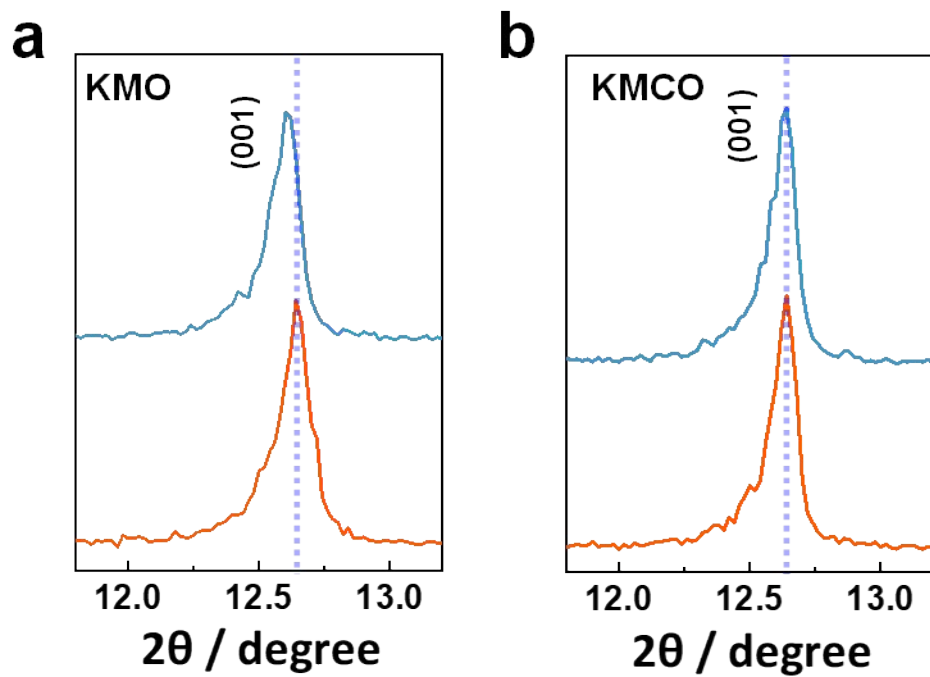


Fig. S13 XRD patterns of (a) KMO and (b) KMCO in the 2θ regions of 11.5° - 13.5° in Fig. 5e and g, respectively.

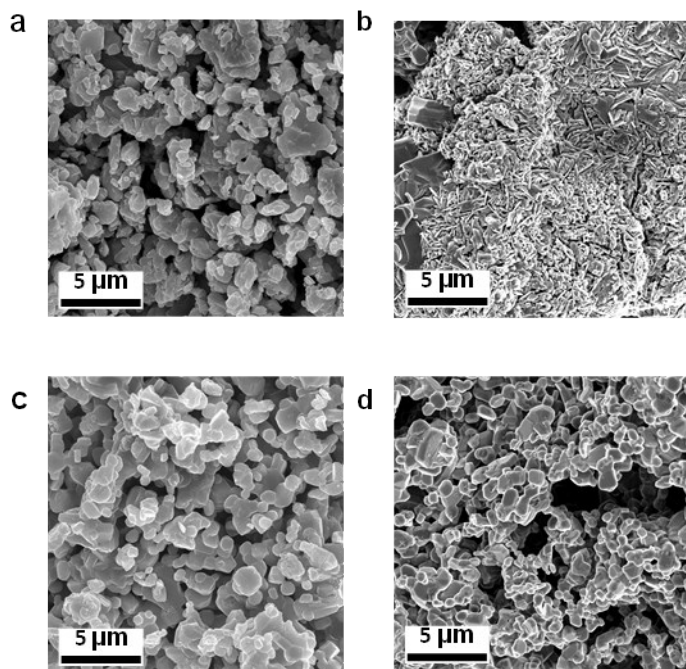


Fig. S14 SEM image of pristine (a) KMO and (c) KMCO, air exposed (b) KMO and (d) KMCO for four weeks.

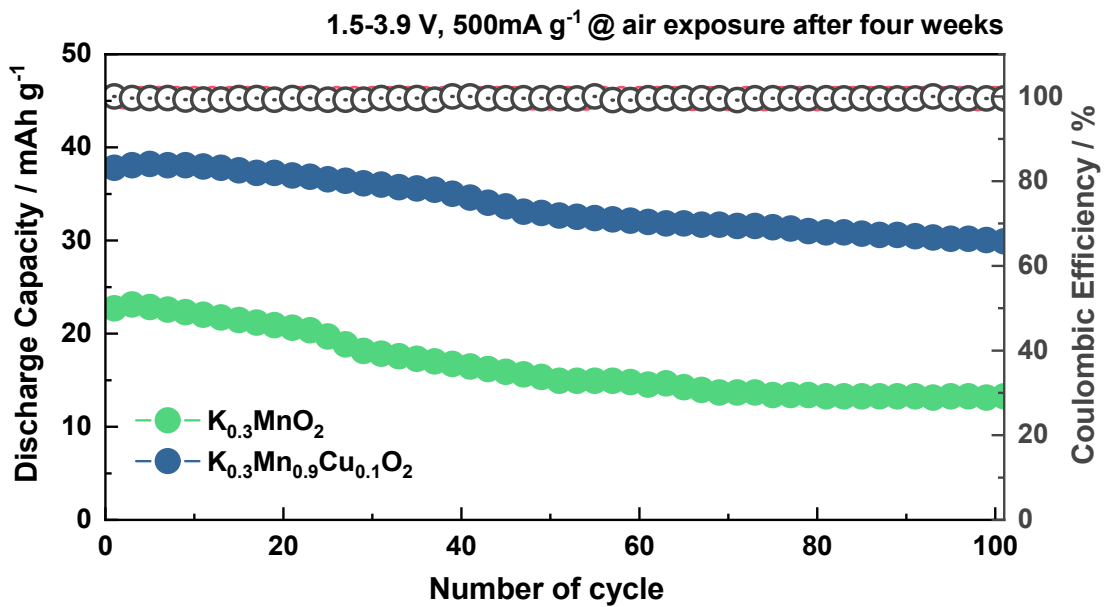


Fig. S15 Cycling stability of KMO and KMCO at 500 mA g⁻¹ after four weeks air exposure.

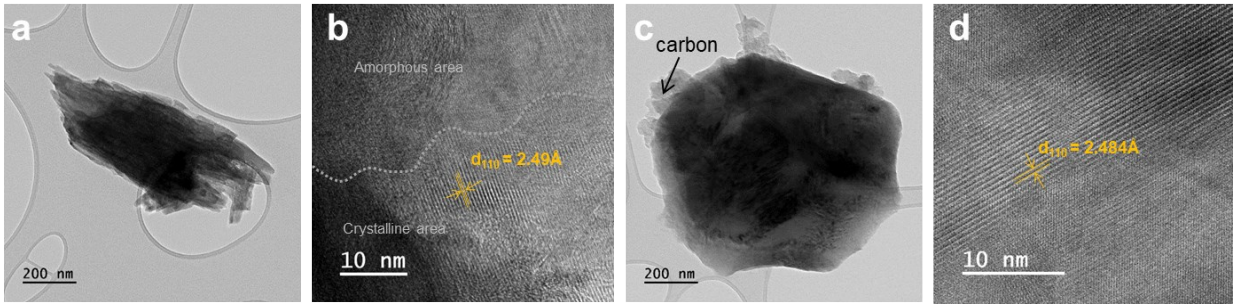


Fig. S16 Bright field TEM images of the (a) cycled KMO and (b) cycled KMCO particles. The (110) plane of HR-TEM images of the (b) cycled KMO and (d) cycled KMCO.

Reference

- 1 J. Gim, V. Mathew, J. Lim, J. Song, S. Baek, J. Kang, D. Ahn, S.-J. Song, H. Yoon and J. Kim, *Sci. Rep.*, 2012, **2**, 946.
- 2 V. Soundharrajan, B. Sambandam, M. H. Alfaruqi, S. Kim, J. Jo, S. Kim, V. Mathew, Y. K. Sun and J. Kim, *J. Mater. Chem. A*, 2020, **8**, 770–778.
- 3 Oliphant, T.E., 2006. A guide to NumPy (Vol. 1, p. 85). USA: Trelgol Publishing.
- 4 Scardapane, S. and Wang, D., 2017. Randomness in neural networks: an overview. *Wiley Interdisciplinary Reviews: Data Mining and Knowledge Discovery*, 7(2), p.e1200.
- 5 Bhojanapalli, S., Wilber, K., Veit, A., Singh Rawat, A., Kim, S., Menon, A. and Kumar, S., 2021. On the Reproducibility of Neural Network Predictions. arXiv e-prints, pp.arXiv-2102.
- 6 P. Giannozzi, et al., QUANTUM ESPRESSO: A modular and open-source software project for quantum simulations of materials, *J. Phys.: Condens. Matter.*, 2009, **21**, 395502.
- 7 J. P. Perdew, A. Ruzsinszky, G. I. Csonka, O. A. Vydrov, G. E. Scuseria, L. A. Constantin, X. Zhou and K. Burke, *Phys. Rev. Lett.*, 2008, **100**, 039902.
- 8 L. Wang, T. Maxisch and G. Ceder, *Phys. Rev. B - Condens. Matter Mater. Phys.*, 2006, **73**, 195107.
- 9 S. Grimme, J. Antony, S. Ehrlich, S. Krieg, A consistent and accurate ab initio parametrization of density functional dispersion correction (dft-d) for the 94 elements H-Pu', *J. Chem. Phys.*, 2010, **132**, 154104.
- 10 K. Momma and F. Izumi, *J. Appl. Crystallogr.*, 2011, **44**, 1272–1276.